

Detection limits of electric field characterization at a p-n junction by 4D-STEM

Bruno Cesar da Silva¹, Yiran Lu¹, Alexis Wartelle¹, Eva Monroy², Jean-Luc Rouviere³, David Cooper⁴, **Dr Martien den Hertog**¹

¹Univ. Grenoble Alpes, CNRS, Grenoble INP, Institut Néel, 38000 Grenoble, France, Grenoble, France, ²Univ. Grenoble-Alpes, CEA, Grenoble INP, IRIG, PHELIQS, Grenoble, France, Grenoble, France, ³Univ. Grenoble-Alpes, CEA-IRIG, MEM, Grenoble, France, Grenoble, France, ⁴CEA, LETI, MINATEC, Grenoble, France, Grenoble, France

The emergence of fast pixelated direct electron detectors over the last years is allowing experiments in four-dimensional scanning transmission electron microscopy (4D-STEM) that would previously be too slow or noisy to be feasible, for example enabling the assessment of internal electric fields with high spatial resolution and precision[1–4] However, the electric field strength of long range built-in electric fields present in semiconductor devices, for example those associated with p-n junctions, is typically three orders of magnitude smaller than atomic electric fields, making 4D-STEM experiments in such systems challenging. It is therefore interesting to assess the detection limit and signal to noise that can be expected depending on the TEM operation conditions.

In this presentation, we describe how the quantification, sensitivity and spatial resolution of electric field mapping in a silicon p-n junction are influenced by the acquisition parameters in a momentum-resolved 4D-STEM experiment [3,5] comparing two different TEM setups differing in brand and in age by 10 years: the first setup, a TFS Titan Ultimate, was installed in 2012; the second, a Jeol Neo Arm in 2022. Both instruments provide 4D STEM capabilities using a Merlin camera based on medipix technology from Quantum Detectors. We have used the center-of-mass approach to analyze the diffraction patterns, obtained on a focused ion beam prepared silicon sample containing a p-n junction.

It will be shown that the success of the quantitative measurements depends not only on the correct estimation of the dead layer, but also on the acquisition conditions, most importantly the electron beam convergence angle.

The detection limit, defined as the three-sigma standard deviation of the field value away from the field containing region, was evaluated both as a function of beam semi-convergence angle as well as TEM setup. It was observed that the electric field precision improves by decreasing the semi-convergence angle [5]. For example, at a convergence angle of about 200 μ rad, the detection limit was as good as 0.01 MV/cm, and it can even be lowered to 0.007 MV/cm in the more recent TEM setup. While such a low convergence angle setting gives the best detection limit and signal to noise ratio of the electric field (SNR 10 and 20, respectively), the increased probe size (estimated around 10 nm) can lead to an underestimation of the electric field value if the field containing region is of similar size as the electron probe. This was the case in the sample under study, where the field containing region was about 50 nm wide. Increasing the convergence angle to about 1 mrad avoids the underestimation of the field since the probe size is smaller (3-4 nm), at the expense of an increased detection limit. With about 1 mrad convergence angle a precision of 0.087 and 0.030 MV/cm with SNR 1.8 and 4.7 were achieved, respectively. As an example, maps of the modulus of the electric field are shown in Fig. 1 together with electric field profiles integrating either over 12 or 90 nm at three different convergence angles, where the Jeol Neo Arm is operated in Lorentz STEM mode.

The effect of electron dose is an important parameter, in particular in relation to beam sensitive materials. The influence of dose was evaluated and invariable electric field profiles were obtained using an electron dose as low as 24 e-/Å. Of course, the precision of the

measurement does depend on dose. It was shown that for an average electron count of about 25 -75 counts per px, the detection limit does not further decrease for increased exposure times. Above this number of counts, the detection limit seems no longer limited by statistical Poisson noise on the detector, but by experimental instabilities, such as fluctuations on the high tension or lens currents or irregularities on the sample such as surface roughness.

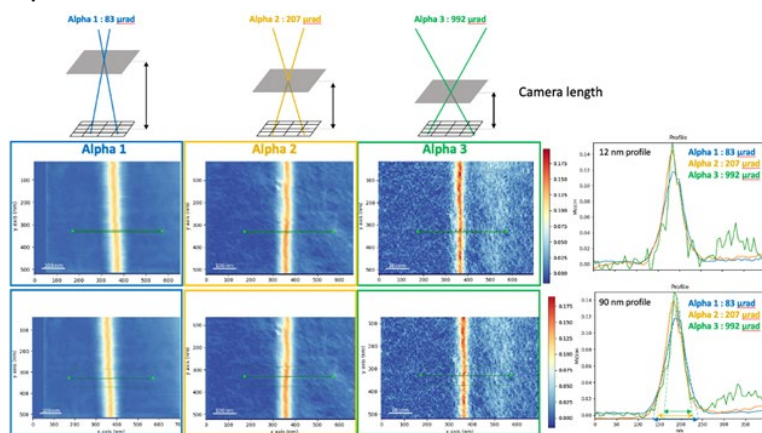
In addition, in-situ electrical biasing coupled to momentum-resolved 4D-STEM measurements were performed, investigating the study of the degree of ideality of the junction abruptness, allowing the detection of phenomena like dopant segregation or interdiffusion [4].

This work paves the way for the development of advanced STEM based techniques able to provide imaging and quantification of built-in electric fields, potentials and charge densities in semiconductor devices with high spatial resolution, providing crucial feedback to improve growth/device fabrication processes.

Figure 1: 4D STEM maps at different convergence angle: The local modulus of the electric field is represented using three different Lorentz STEM modes of the Jeol Neo Arm, with three different convergence angles. Profiles are made along 12 nm, top row, and along 90 nm, bottom row.

Acknowledgements: This project received funding from the European Research Council under the European Union’s H2020 Research and Innovation programme via the e-See project (Grant No. 758385). Experiments have been performed at the Nanocharacterisation platform PFNC in Minatec, Grenoble as well as at TEM facility JEOL NEOARM co-financed by the European Union under the European Regional Development Fund (ERDF, contract n° RA0023813).

Graphic:



Keywords:

4D-STEM, electric field characterization, biasing

Reference:

- [1] L. Bruas, et al, J. Appl. Phys. 2020, 127, 205703.
- [2] A. Beyer, et al, Nano Lett. 2021, 21, 2018–2025.
- [3] B. C. da Silva, et al, Appl. Phys. Lett. 2022, 121, 123503.
- [4] B. C. da Silva, et al, Nano Lett. 2022, 22, 9544–9550.
- [5] S. Pöllath, et al, Ultramicroscopy 2021, 228, 113342.